

# Formation and Self-Assembly of Coherent Quantum Dots: Some Thermodynamic Aspects

**José Emilio Prieto**

Centro de Microanálisis de Materiales and  
Instituto Universitario de Ciencia de Materiales “Nicolás Cabrera”,  
Universidad Autónoma de Madrid, 28049 Madrid, Spain

**Elka Korutcheva**

Dpto. de Física Fundamental, UNED, Senda del Rey 9, 28080 Madrid, Spain

**Ivan Markov**

Institute of Physical Chemistry, Bulgarian Academy of Sciences, 1113 Sofia,  
Bulgaria

## Abstract

Quantum dots have promising properties for optoelectronic applications. They can be grown free of dislocations in highly mismatched epitaxy in the coherent Stranski-Krastanov mode. In this chapter, some thermodynamic aspects related to the wetting in the growth and self-assembly of three-dimensional (3D) coherent islands are studied using an energy minimization scheme in a 1+1-dimensional atomic model with anharmonic interactions. The conditions for equilibrium between the different phases are discussed. It is found that the thermodynamic driving force for 3D-cluster formation is the reduced adhesion of the islands to the wetting layer at their edges. In agreement with experimental observations, for values of the lattice mismatch larger than a critical misfit, a critical island size for the 2D-3D transition is found. Beyond it, monolayer islands become unstable against bilayer ones. Compressed coherent overlayers show a greater tendency to clustering than expanded ones. The transition to 3D islands takes place through a series of intermediate stable states with thicknesses discretely increasing in monolayer steps. Special emphasis is made on the analysis of the critical misfit. Additionally, the effect of neighbouring islands mediated through a deformable wetting layer is considered. The degree of wetting of the substrate by a given island depends on the size and shape distributions of the neighbouring islands. Implications for the self-assembled growth of quantum dots are discussed.

## 1 Introduction

The fabrication of ordered arrays of self-assembled, three-dimensional (3D) nano-sized islands is the subject of intense research in recent times due to their possible applications in the fields of nanomagnetism and optoelectronics.[1] To obtain semi-conducting “quantum dots” that can be efficiently used as lasers and light-emitting diodes, it is convenient to grow islands which are *coherent* with the atomic layers underneath, i.e., that do not contain misfit dislocations (MDs). One promising

approach to the fabrication of such structures is to exploit the “coherent Stranski-Krastanov (SK) growth” in the epitaxy of highly mismatched materials. This case is different from the “classical” SK growth in which the lattice mismatch is accommodated by MDs at the interface with the wetting layer.[2] The term “coherent” SK growth has been coined for this case of formation of 3D islands that are strained to fit the underlying strained wetting layer of the same material at the interface but are largely strain-free near their top and side walls.[3, 4] It has been recently reported in a series of systems, e.g. Ge on Si,[3, 5, 6, 7, 8, 9, 10, 11] InAs on GaAs,[12, 13, 14, 15, 16, 17] InGaAs on GaAs,[18, 19, 20, 21] InP on  $\text{In}_{0.5}\text{Ga}_{0.5}\text{P}$ ,[22] that coherently strained (dislocation-free) 3D islands grow on the wetting layer. In all these cases, the lattice misfit is positive and very large (4.2, 7.2 and about 3.8 % for Ge/Si, InAs/GaAs and InP/ $\text{In}_{0.5}\text{Ga}_{0.5}\text{P}$ , respectively) for semiconductor materials, which are characterized by directional and brittle chemical bonds. A possible (partial) exception might be the system PbSe/PbTe(111), where the misfit is negative (-5.5 %) and the overlayer is expanded.[23]

The growth of thin epitaxial films takes place usually in conditions far from equilibrium, particularly when using deposition methods in vacuum like molecular beam epitaxy. Nevertheless, thermodynamic considerations are a necessary step to understand many aspects of the growth process. Of particular interest for the case of the coherent SK growth is the thermodynamic driving force (TDF) responsible for the 3D islanding. The reason is that we have in fact the growth of  $A$  on strained  $A$ , the coherent 3D islands being strained to the same degree as the wetting layer. A naive conclusion from this would be that the energy of the interfacial boundary between the 3D islands and the wetting layer is equal to zero. Although this energy is certainly expected to be small compared to the free energy of the crystal faces involved [1], it cannot be neglected since this would imply that the islands wet completely the wetting layer, ruling out 3D islanding from a thermodynamic point of view [24].

The need for a thermodynamic analysis arises also from the experimental observation of a critical misfit for coherent 3D islanding,[18, 23, 25, 26] and the simultaneous presence of islands of different thicknesses which vary by one monolayer (ML).[27, 28] The existence of a critical misfit, as well as of stable two-, three- or four-ML-thick islands, do not follow from the tradeoff [1, 29]

$$\Delta E \approx C' \gamma V^{2/3} - C'' \varepsilon_0^2 V \quad (1)$$

between the cost of the additional surface energy and the gain of energy due to the elastic relaxation of the 3D islands relative to the wetting layer ( $V$ ,  $\gamma$  and  $\varepsilon_0$  are the islands volume, the specific surface energy and the lattice misfit, respectively, and  $C'$  and  $C''$  are constants).

For these reasons, in this chapter we first recall some simple thermodynamic aspects of the epitaxial morphology based on the traditional concept of wetting and consider the coherent SK growth from this point of view. The basic ideas are

then supported by numerical calculations that make use of a simple model in 1 + 1 dimensions with anharmonic interactions.

In order for the 3D islands to be useful for technical applications, they have to be produced with high areal densities and with a high degree of similarity and homogeneity. Experimental studies of arrays of coherent 3D islands of highly mismatched semiconductor materials have shown surprisingly narrow size distributions.[12, 18, 30, 31] This phenomenon, known as self-assembly,[32] is highly desirable as it guarantees a specific optical wavelength of the array of quantum dots.

In the second part of this chapter, we address the topic of self-assembly. We consider no longer single isolated islands, but groups of islands on top of a deformable wetting layer consisting of several atomic planes that are allowed to relax in response to the strain fields produced by the misfitting islands. In this way, elastic interactions between the islands can be studied. We will focus on the wetting of islands that are part of an array, i.e., that are surrounded by neighbouring islands. We study the effect of the density of the array (the distance to the nearest neighbouring islands), the size distribution (the difference in size of the neighbouring islands) and the shape distribution (the slope of the side walls of the neighbouring islands) on the wetting parameter  $\Phi$  of the considered island. The results are finally discussed and compared to experiments.

## 2 Wetting in the coherent SK growth

We consider two different phases. The first is one which we can call a mother or ambient phase. We can think of it as the vapour phase. The second is a condensed phase and can consist either of a strained planar film or of unstrained 3D crystals. A fundamental thermodynamical result is that two phases are in equilibrium with each other when their chemical potentials are equal. A transition from one phase to a second one takes place when the chemical potential of the second becomes smaller than that of the first. The TDF for the transition is thus the difference of the chemical potentials of both phases at the given pressure and temperature. Therefore, the TDF which determines the occurrence of one or another mechanism of epitaxial growth (i.e., the growth of a coherently strained 2D layer or of 3D crystallites) is the difference

$$\Delta\mu = \mu(n) - \mu_{3D}^0 \quad (2)$$

of the chemical potential of the overlayer  $\mu(n)$ , which depends on the average film thickness (measured in number  $n$  of monolayers counted from the interface), and the chemical potential,  $\mu_{3D}^0$ , of the bulk 3D crystal of the same material.[33, 34, 35]

The thickness dependence of the film chemical potential  $\mu(n)$  originates from the thickness distribution of the misfit strain and from the interaction between the deposit and the substrate, which rapidly decreases with the distance from the interface and can usually be neglected beyond several MLs.[33, 34, 35]

We can describe the essential phenomenology in terms of the wetting considering a simple model of epitaxial growth of a crystal A on a substrate B. At this stage, we do not include any lattice misfit between the two materials but only a difference in the strength of the chemical bonding.

As is well known, the wetting parameter which accounts for the energetic influence of the crystal B on A is defined as (for a review see Ref. [36])

$$\Phi = 1 - \frac{E_{AB}}{E_{AA}}, \quad (3)$$

where  $E_{AA}$  and  $E_{AB}$  are the energies per atom required to disjoin a half-crystal A from a like half-crystal A and from an unlike half-crystal B, respectively.

The chemical potential of the bulk crystal A is given at zero temperature by  $-\phi_{AA}$ , where  $\phi_{AA}$  is the work required to detach an atom from the well known kink or half-crystal position. This name is due to the fact that an atom at this position is bound to a half-atomic row, a half-crystal plane and a half-crystal block.[37, 38] In the case of a monolayer-thick film of A on the surface of B, the chemical potential of an atom A is given by the analogous term  $-\phi_{AB}$  whereby the underlying half-crystal block of A has been replaced by a half-crystal block of B. Therefore we have

$$\Delta\mu = \phi_{AA} - \phi_{AB}. \quad (4)$$

In the simplest case of additivity of the energies of lateral and vertical bonds, this difference reduces to  $E_{AA} - E_{AB}$  as the lateral bondings cancel each other (it is easy to show that Eq. 4 is equivalent to the well known 3- $\sigma$  criterion of Bauer [39, 36]). Then  $\Delta\mu$  is proportional to  $\Phi$ : [36]

$$\Delta\mu = E_{AA}\Phi. \quad (5)$$

It follows that it is in fact the wetting parameter  $\Phi$  which determines the mechanism of growth of A on B[24] as illustrated by Figure 1. We first consider two limiting cases. The Volmer-Weber (VW) growth of isolated 3D islands of A on the surface of B takes place at any misfit  $\varepsilon_0$  and is characterized by the incomplete wetting of the substrate ( $0 < \Phi < 1$ ). The value of  $\Delta\mu$  is always positive and decreases asymptotically to zero with increasing thickness. The opposite limit is the consecutive formation of MLs of A on B in the Frank - van der Merwe (FW) growth, with complete wetting ( $\Phi \leq 0$ ). For this mode of growth is required that  $\varepsilon_0 \approx 0$ . In this case,  $\Delta\mu$  is always negative and tends asymptotically to zero with increasing thickness.

Also shown in Figure 1 is the intermediate and important case of the SK mode of growth, which takes place when the atoms of the deposit bind stronger to those of the substrate than to themselves ( $E_{AB} > E_{AA}$ ) but the lattice misfit  $\varepsilon_0$  is substantial. The first condition causes a complete wetting at the beginning of the growth ( $\Phi < 0$ ) but the second produces an accumulation of strain energy with increasing film thickness which turns the balance towards  $\Phi > 0$  (incomplete wetting) at some

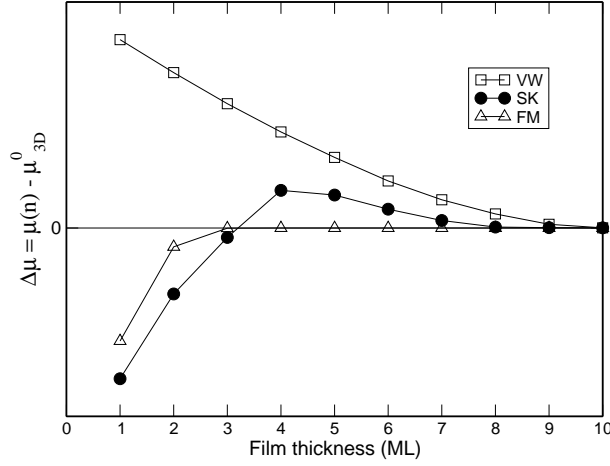


Figure 1: Schematic dependence of the film chemical potential on the film thickness in monolayers for the three classical modes of growth: VW – Volmer-Weber, SK – Stranski-Krastanov, and FM – Frank-van der Merwe.

value of the thickness  $n$ . In the classical SK growth, the introduction of MDs allows for a release of strain energy through a structural relaxation of the film and to the development of 3D islands.

It is instructive to consider also Fig. 1 in terms of equilibrium vapour pressures. Although the connection with the chemical potential is straightforward ( $\mu \propto \ln P$ ), this gives a deeper insight into the problem. Thus, as long as  $\mu(n) < \mu_{3D}^0$  a thin planar film can be deposited at a vapour pressure  $P$  smaller than the equilibrium vapour pressure  $P_0$  of the bulk crystal, but larger than the equilibrium vapour pressure  $P_1$  of the first ML, i.e.  $P_1 < P < P_0$ . In other words, a planar film can be deposited at *undersaturation*  $\Delta\mu = kT \ln(P/P_0)$  with respect to the bulk crystal. The formation of 3D islands [ $\mu(n) > \mu_{3D}^0$ ] requires  $P > P_0$ , or a *supersaturation* with respect to the bulk crystal. We thus conclude that the 3D islands and the wetting layer represent necessarily different phases and thus have different chemical potentials. The reason is that the two phases are in equilibrium with the mother phase under different conditions which never overlap.[40] The wetting layer can be in equilibrium only with an undersaturated vapour phase ( $P < P_0$ ), while small 3D islands can be in equilibrium only with a supersaturated vapour phase ( $P > P_0$ ). The dividing line is thus  $\Delta\mu = kT \ln(P/P_0) = 0$  at which the wetting layer cannot grow thicker and the 3D islands cannot nucleate and grow. Hence the wetting layer and the 3D islands can never be in equilibrium with each other.

The derivative,  $d\Delta E/dV$ , of the energy of the 3D islands relative to that of the wetting layer, gives the difference of the chemical potentials of the wetting layer and the chemical potential of the 3D islands. In other words, it represents the difference of the supersaturations of the vapour phase with respect to the wetting layer and the

3D islands. Transfer of material from the stable wetting layer defined by  $\mu_{\text{WL}} < \mu_{\text{3D}}^0$  to the 3D islands is connected with an increase of the free energy of the system and therefore is thermodynamically unfavoured. A planar film thicker than the stable wetting layer is unstable and the excess of the material must be transferred to the 3D islands if the necessary thermal activation exists.

The Stranski-Krastanov morphology appears as a result of the interplay of the film-substrate bonding, misfit strain and the surface energies. A wetting layer with a thickness of the order of the range of the interatomic forces is first formed (owing to the interplay of the A-B interaction and the strain energy accumulation) on top of which partially or completely relaxed 3D islands nucleate and grow. The 3D islands and the thermodynamically stable wetting layer represent necessarily different phases. If this were not the case, the growth would continue by 2D layers. Thus we can consider as a useful approximation to regard the 3D islanding on top of the uniformly strained wetting layer as a Volmer-Weber growth. That requires the mean adhesion of the atoms that belong to the base plane of the 3D islands to the stable wetting layer to be smaller than the cohesion between them. In other words, the wetting of the underlying wetting layer by the 3D islands must be incomplete. Otherwise, 3D islanding will not occur.[24] In the Volmer-Weber growth the incomplete wetting is due mainly to the difference in bonding ( $E_{\text{AB}} < E_{\text{AA}}$ ), the supplementary effect of the lattice misfit being usually smaller. In the classical SK growth, the incomplete wetting is due to the energetic cost of the array of MDs.

In view of this, the case of *coherent* SK growth seems difficult to understand, since in the absence of MDs there is no obvious difference between the atoms of the wetting layer and those of the islands. If this is so, then there is no evident reason for the consideration of two different phases, the wetting must be complete and 3D islanding should not occur.[24]

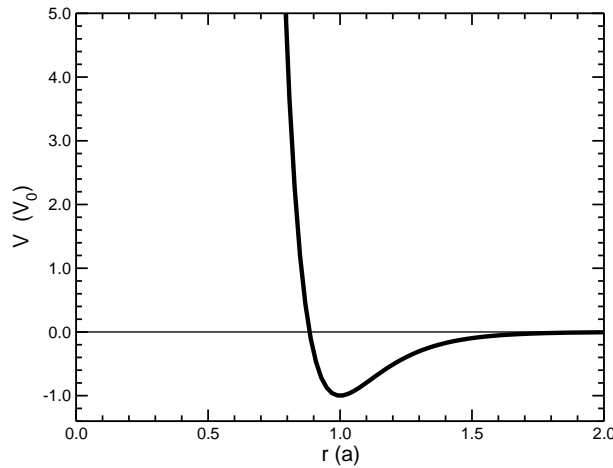


Figure 2: Graphical representation of the atomic interaction potential, of the Morse type, used in the calculations in this work.

It has been recently suggested that the TDF for the *coherent* SK growth, where  $E_{AB} \approx E_{AA}$ , is the incomplete wetting of the substrate by the islands.[41] The origin of the reduced adhesion are the displacements of the atoms near the island edges from the bottoms of the corresponding potential troughs provided by the wetting layer underneath. However, the approximation used by the authors, which is based on the 1D model of Frenkel and Kontorova,[42, 43] is unable to describe correctly the individual behaviour of atoms inside each layer, since it assumes a potential with a period given by the average of the separations of atoms (considered frozen) in the layer underneath. Although this model gives qualitatively reasonable results concerning the energy of the islands, it is inadequate to calculate, in particular, the structure and energy of the interfacial boundary between the wetting layer and the 3D islands upon thickening of the latter. The model is further unable to consider the effect of neighbouring islands on the wetting of a given one.

## 2.1 Model

For the above-mentioned reasons, we have performed atomistic calculations making use of a simple minimization procedure. The atoms interact through a pair potential whose anharmonicity can be varied by adjusting two constants  $\mu$  and  $\nu$  ( $\mu > \nu$ ) that govern separately the repulsive and the attractive branches, respectively,[44]

$$V(x) = V_o \left[ \frac{\nu}{\mu - \nu} e^{-\mu(x-a)} - \frac{\mu}{\mu - \nu} e^{-\nu(x-a)} \right], \quad (6)$$

where  $a$  is the equilibrium atom separation. For  $\mu = 2\nu$  the potential (6) turns into the familiar Morse form, which has been used in the present work for the particular case  $\nu = 6$ . This potential is shown in Figure 2.

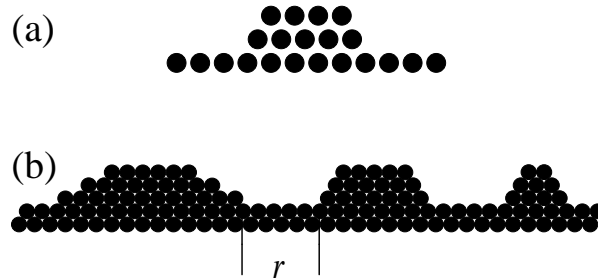


Figure 3: Schematic view of (a) an isolated island on a rigid substrate with side angles of  $60^\circ$  and (b) an array of islands on a wetting layer. The central island is surrounded by two islands with different shapes and sizes. The distance between neighbouring islands is given by  $r$ .

Our programs calculate the interaction energy of all the atoms as well as its gradient with respect to the atomic coordinates, i.e. the forces. Relaxation of

the system is performed by allowing the atoms to displace in the direction of the gradient in an iterative procedure until the forces fall below some negligible cutoff value. The calculations for isolated islands were performed under the assumption that the substrate (the wetting layer) is rigid. It was carefully checked that removing this restriction, i.e., allowing several layers below the islands to relax did not change qualitatively the results.

We consider an atomistic model in  $1 + 1$  dimensions which can be regarded as a cross-section of the real  $2 + 1$  case. An implicit assumption is that the islands have a compact rather than a fractal shape and that the lattice misfit is the same in both orthogonal directions. The 3D islands are represented by linear chains of atoms stacked one upon the other [42] as shown schematically in Fig. 3(a). The shape of the islands in our model is given by the slope of the side walls.

In the case of arrays of islands, the restriction of a rigid substrate must obviously be lifted in order for it to mediate elastic interactions between the islands. The  $1+1$ -dimensional array is represented by a row of 3 (occasionally 5) islands on a wetting layer consisting of several MLs which are allowed to relax. The distance between two neighbouring islands is given by the number  $r$  of vacant atomic positions between the ends of their base chains, as illustrated by Fig. 3(b). Periodic boundary conditions are applied in the lateral direction.

For the sake of simplicity in the computational procedure, we consider in our model a wetting layer that is in fact composed of several MLs of the true wetting layer of the overlayer material A plus several MLs of the unlike substrate material B. This “composite wetting layer” has the atom spacing of the substrate material B as in the real case, but the atom bonding of the overlayer material A. This underestimates somewhat the value of  $\Phi$ , because the A-A bonding is necessarily weaker than the B-B bonding in order for SK growth to be possible, but it does not introduce a significant error since the energetic influence of the substrate B is screened by the true wetting layer A.

In the present work, we will be primarily concerned with the wetting. It is therefore important to define precisely the wetting parameter  $\Phi$ . In the coherent SK the relation between  $\Delta\mu$  and  $\Phi$  is not as simple as that given by Eq. 5, because the bond energies are generally not additive, the misfit strain is relaxed mostly near the side and top walls and increasing the island thickness leads to larger displacements of the edge atoms, as will be shown below. For these reasons, in this work we define the wetting parameter  $\Phi$  as the difference of the interaction energies with the wetting layer of misfitting and non-misfitting 3D islands.

## 2.2 Atomistics at the interface

We first consider the characteristics of the adhesion between the *coherent* 3D islands and the wetting layer. Fig. 4(a) shows the horizontal displacements of the atoms of the base chain. They are measured from the bottoms of the corresponding potential troughs of the wetting layer. It can be seen that the end atoms are strongly displaced

as in the model of Frenkel and Kontorova,[43] and of Frank and van der Merwe.[45] Increasing the island height leads to larger displacements of the end atoms. The reason is the effective increase of the strength of the lateral interatomic bonding in the overlayer with greater thickness as predicted by van der Merwe *et al.*[46] Fig. 4(b) shows the vertical displacements of the base-chain atoms relative to the interplanar spacing between the MLs belonging to the wetting layer. The vertical displacements are obviously due to the climbing on top of the underlying atoms as a result of the horizontal displacements. The thicker the island, the larger the horizontal and, in turn, the vertical displacements. The consequence is that the island loses contact with the underlying wetting layer.

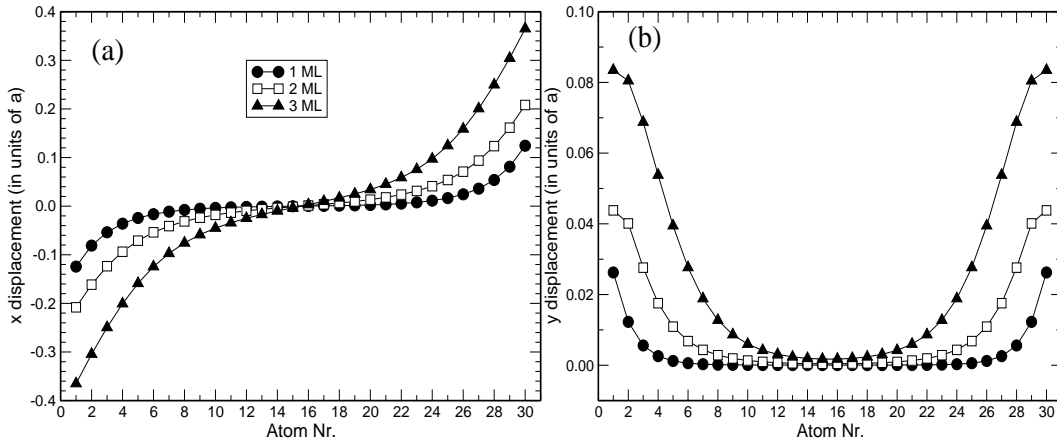


Figure 4: Horizontal (a) and vertical (b) displacements of the atoms of the base chain from the bottoms of the potential troughs provided by the homogeneously strained wetting layer for a misfit of 7.0 %. The displacements are given in units of  $a$ , the lattice parameter of the substrate and wetting layer, for different island thicknesses. Islands of 30 atoms in the base chain were considered.

It is instructive to compare these atomic displacements in coherently strained islands with those found in the *classical* SK growth. For this case, the interconnection between vertical and horizontal displacements is shown in Fig. 5(a) for an island containing two MDs. The horizontal displacements are now larger in the cores of the MDs and so are also the vertical displacements. Figure 5(b) is a further illustration of the differences and resemblances between the classical and the coherent SK modes. It shows the vertical displacements for both types of 3D islands. The sizes of the base chain of the islands (30 and 34 atoms, respectively) are just below and above the critical size for introduction of misfit dislocations at the given values of the thickness (3 ML) and the lattice misfit (7.0 %). As seen, in both cases the 3D islands loose contact with the wetting layer. The vertical displacements are largest at the chain's ends in the coherent SK mode and around the dislocation cores in the classical case, but the physics is essentially the same. In both cases we find a

reduction of the adhesion which leads to the 3D islanding.

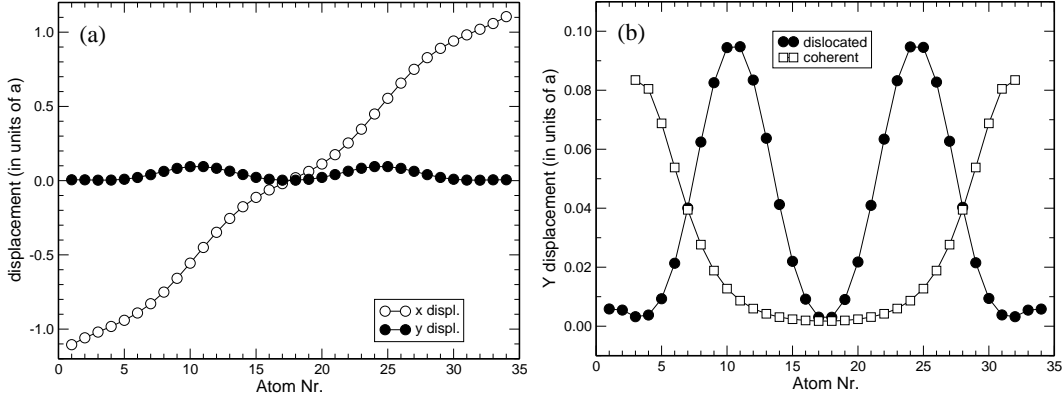


Figure 5: (a): horizontal (x) and vertical (y) displacements of the atoms of the base chain of a 3 ML-thick island that contains two MDs. The island has a total amount of 99 atoms (34 in the base chain) and the lattice misfit is 7.0 %. The vertical displacements are shown in an enlarged scale in (b), together with those of a coherent island of the same thickness and 30 atoms in the base chain. Displacements are given in units of the lattice parameter of the wetting layer and are measured from the bottoms of the potential troughs provided by it.

The power of our atomistic approach is that it allows us to study the behaviour of the individual atoms that form an island. In order to illustrate the effect of the atom displacements on the adhesion of the separate atoms belonging to the island base chain, we have plotted their energy of interaction with the underlying wetting layer in Fig. 6 for coherently strained islands with values of the misfit of +7.0 % and -7.0 %. It can be seen that the atoms that are closer to the island's edges adhere weaker to the substrate. The influence of the potential anharmonicity is also clearly demonstrated. Only one or two end atoms in the expanded chain adhere weaker to the substrate whereas more than half of the atoms at both ends do so in the compressed chain. The figure demonstrates in fact the physical reason for the coherent SK mode which is often overlooked in theoretical models. Moreover, it is a clear evidence of why compressed rather than expanded overlayers exhibit greater tendency to coherent SK growth.

Another consequence of the atomic displacements shown in Fig. 4 is that increasing the islands thickness leads to a weaker adhesion with the wetting layer and, in turn, to a stabilization of the coherent 3D islands. This is demonstrated in Fig. 7, which shows the dependence of the mean adhesion parameter  $\Phi$  on the island height. As seen it saturates beyond a thickness of about 5 ML. This effect has been predicted recently by Korutcheva *et al.*[41] by using the approximation suggested by van der Merwe *et al.*[46]

The same tendency is demonstrated even more clearly in Fig. 8 where the mean adhesion parameter of coherent monolayer-high islands is plotted as a function of

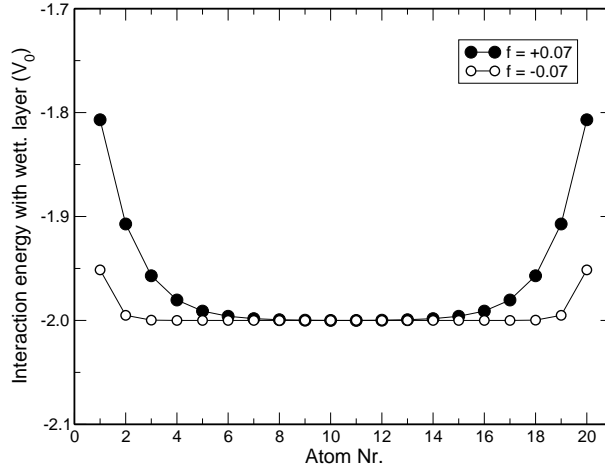


Figure 6: Distribution of the energy (in units of  $V_0$ ) of first-neighbours interaction between the atoms of a monolayer-high coherent island of 20 atoms and the underlying wetting layer, for positive and negative misfits of absolute value 7.0 %.

the lattice misfit in both cases of compressed and expanded overlayers. In fact the figure shows the TDF  $\Delta\mu$  for the transformation of monolayer-high islands into 3D islands. The wetting parameter increases very slowly and is nearly equal to zero up to about 12 % for expanded overlayers, whereas it increases steeply beyond a value of the misfit of approximately 5 % in compressed overlayers. As will be shown below, this is in agreement with the misfit dependence of the critical size (volume) for the mono-bilayer transformation to occur.

An additional proof that the TDF for coherent 3D islanding is the reduced adhesion is obtained by studying the energies of 2D and 3D islands as a function of the total number of atoms or the volume. A direct consequence of such a study is the existence of a critical misfit beyond which coherent 3D islanding can take place. We compare the energies per atom of mono- and multilayer high islands with different thickness increasing discretely by one monolayer. One of the reason for doing this is that islands with different thickness have different adhesion parameters (see Fig. 7). Moreover, as shown by Stoyanov and Markov, such an approach originates from the classical concept of minimum of the surface energy at a fixed volume.[47] It is particularly applicable to small crystallites formed on unlike surfaces where the crystal height is a discrete rather than a continuous variable.

Fig. 9(a) shows the energies per atom plotted as a function of the total number of atoms in coherent monolayer- and bilayer-high islands at  $\varepsilon_0 = 3.0$  %. As seen, the monolayer islands are always stable against the bilayer islands. This means that thermodynamics does not favour coherent 3D islanding. Monolayer-high islands will grow and coalesce until they cover the whole surface. Misfit dislocations will be then introduced to relieve the strain. The reason for this behaviour is clearly

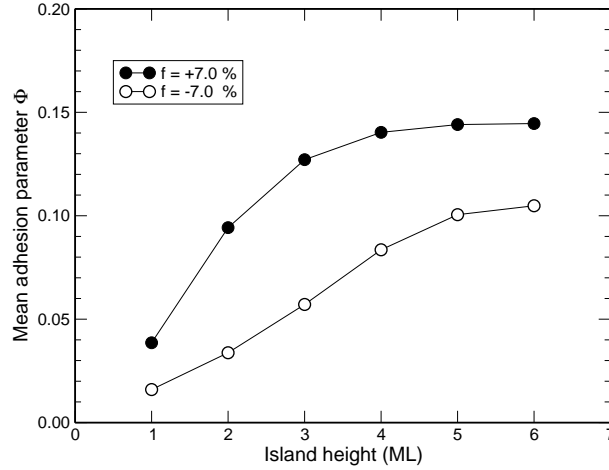


Figure 7: Mean adhesion parameter  $\Phi$  as a function of the islands' height in number of MLs for positive and negative values of the misfit of absolute value of 7.0 %. Coherent islands of 14 atoms in the base chain were considered in the calculations.

the negligible value of the adhesion parameter as shown in Fig. 8. Figure 9(b) demonstrates the same dependence (including also thicker islands) for a larger value of the misfit  $\varepsilon_0 = 7.0\%$ , at which the adhesion parameter has clearly a non-zero value. This time the behaviour is completely different. Monolayer islands are stable against bilayer islands only up to a critical volume  $N_{12}$ , the bilayer islands are stable in turn against the trilayer islands up to a second critical volume  $N_{23}$ , etc.[48] This behaviour is precisely the same as in the case of VW growth where the interatomic forces  $AA$  and  $AB$  differ and the lattice misfit plays an additional role.[47] The same result (not shown) has been obtained in the case of expanded overlayers ( $\varepsilon_0 < 0$ ) with the only exception that monolayer-high islands are stable against multilayer islands up to much larger absolute values of the misfit.

Figure 9(b) suggests that the mono-bilayer transformation appears as the first step of the complete 2D-3D transformation. The dependence of the critical size  $N_{12}$  on the lattice misfit, as shown in Fig. 10, shows the existence of critical misfits only beyond which the formation of multilayer islands can take place. Below the critical misfit the monolayer-high islands are stable irrespective of their size and the growth will continue in a layer-by-layer mode until misfit dislocations are introduced at the interface to relax the strain. The much larger absolute value of the negative critical misfit is obviously due to the anharmonicity of the atomic interactions. The weaker attractive interatomic forces lead to smaller displacements, both lateral and vertical, of the end atoms and in turn to stronger adhesion. Thus, a larger misfit is required in order for 3D islanding to take place.

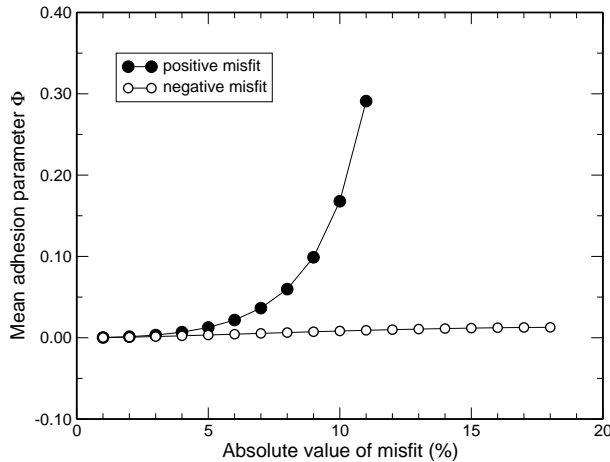


Figure 8: Mean adhesion parameter as a function of the lattice misfit for coherent, 1 ML-thick islands containing 20 atoms. Data for both positive and negative misfits are shown in the same quadrant for easier comparison.

### 3 Self-assembly

The atomic displacements in an island that belongs to an array of islands are shown in Fig. 11. Panel (a) shows the horizontal displacements of the atoms of the base chain from the bottoms of the potential troughs provided by the homogeneously strained wetting layer for a misfit of 7.0 %. The considered island has two identical neighbours at both sides at a distance of  $r = 5$ . This is the same behaviour as predicted by the one-dimensional model of Frank and van der Merwe.[45] The horizontal displacements increase with increasing island thickness (measured in number of MLs) precisely as in the case of a rigid substrate and non-interacting islands (see Fig. 4). But, in contrast to this case, now the vertical displacements of the edge atoms of the base chain of the islands and the underlying atoms of the uppermost ML of the wetting layer are directed downwards, as shown in Fig. 11(b). A similar result has been found by Lysenko *et al.* in the case of homoepitaxial metal growth by means of a computational method based on the tight-binding model.[49]

In spite of their downwards vertical displacements, the edge atoms are again more weakly bound to the underlying wetting layer, as in the rigid substrate case (Fig. 4). This is nicely illustrated in Fig. 12. Shown in the same figure for comparison is also an island without neighbours on the same relaxed wetting layer. It can be seen in both cases that the edge atoms bind weaker than the central atoms to the underlying wetting layer. Compared to an isolated island, the edge atoms of an island in an array adhere weaker to the substrate. Thus the essential physical effect exerted by neighbouring islands on a give one is the additional loss of contact of the latter with the substrate: the wetting parameter must increase.

The behaviour of the wetting parameter as a function of the density of the array is

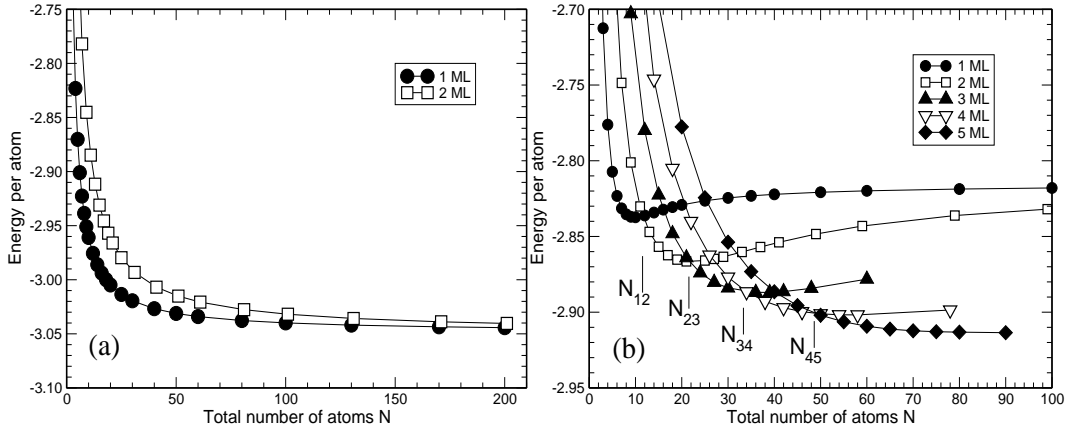


Figure 9: Dependence of the energy per atom, in units of  $V_0$ , on the total number of atoms in compressed, coherently strained islands of different thicknesses for two different values of the misfit: (a) 3.0 %, (b) 7.0 %. The numbers  $N_{12}$ ,  $N_{23}$ , etc. give the limits of stability of monolayer, bilayer... islands, respectively.

illustrated in Fig. 13. As expected, the wetting parameter increases with increasing array density. This figure also allows us to estimate the size of the effect. At a distance  $r=10$  (about 3 nm), neighbours make  $\Phi$  increase by 10 %; this represents an effective decrease in adhesion  $\Delta E_{AB}$  of  $0.10 \Phi E_{AA}$ . For Ge/Si(100) (desorption energy of Ge: 4 eV), this gives about 20 meV, a contribution of the same order as the elastic energy per atom (40 meV in this system [36]) that can significantly affect the delicate balance of the energies involved in the growth process: diffusion barriers and surface/interface energies.

The size distribution of the neighbouring islands is expected to be an important factor affecting the wetting of the island. Figure 14 shows the dependence of the wetting parameter of the central island on the size of the side islands for two different configurations. In the first [Figure 14(a)], the two side islands have identical sizes. Increasing their volume leads to an increase of the elastic fields around them and to a further reduction of the bonding between the edge atoms of the central island and the wetting layer. Figure 14(b) shows the behaviour of the wetting parameter  $\Phi$  of the central island as a function of the number of atoms in the base chain of the left island, whereby the sum of the total number of atoms of left and right islands has been kept constant at precisely the doubled number of the central island. The facet angles of all three islands are always  $60^\circ$ . Thus the first (and, by symmetry, also the last) point give the maximum asymmetry in the size distribution of the array, the left (right) island containing 9 atoms and the right (left) island 105. All three islands are 3 ML thick. The point at the maximal wetting corresponds to the monodisperse distribution: i.e., when the three islands have one and the same volume of 57 atoms. This means that in the case of perfect self-assembly of the array, the wetting parameter and therefore the tendency to clustering display a maximum

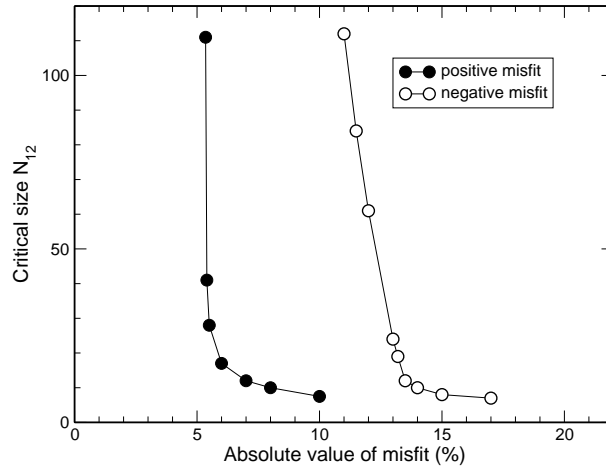


Figure 10: Misfit dependence of the critical size  $N_{12}$  (in number of atoms) for positive and negative values of the lattice misfit. The curves are shown in one quadrant for easier comparison.

value.

As a further parameter affecting the wetting of an island, the influence of the shape of the side islands, i.e. their facet angles, on the wetting parameter of the central island is demonstrated in Fig. 15. The central island is compact, having facet angles of  $60^\circ$ . The effect is greatest when the side islands have the steepest walls. The same result (not shown) is obtained for different shapes of the central island. The explanation follows the same line as the one given above. The islands with larger-angle side walls exert a greater elastic effect on the substrate and in turn on the displacements and the bonding of the edge atoms of the central island.

The effect of the neighbours on the stability of islands with a thickness increasing by one monolayer is illustrated in Fig. 16. The total energy for islands inside an array shows the same behaviour as for isolated islands. This means that also in the case of a deformable substrate, the overall transformation from the precursor 2D islands to the 3D islands takes place in consecutive stages in each of which the islands thicken by one monolayer. The energies computed in the case of the reference single islands always lie below the curves of the islands in an array. The difference obviously gives the energy of repulsion between the neighbouring islands. It follows that the presence of neighbouring islands leads to a slight decrease of the critical misfit and in turn to a greater tendency to clustering.

## 4 Discussion

For the discussion of the above results we have to bear in mind that a positive value of the wetting parameter implies in fact a tendency of the deposit to form 3D

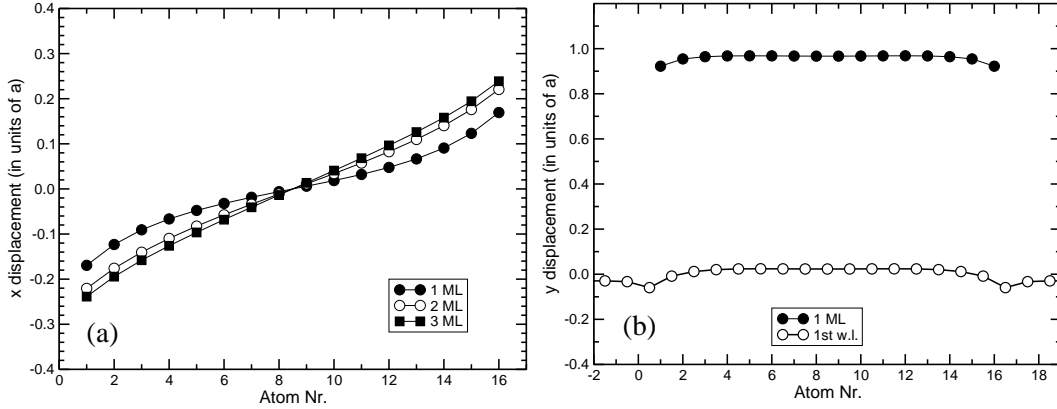


Figure 11: (a): horizontal displacements of the atoms of the base chain for a lattice misfit of 7.0 % and the given island thicknesses. The considered islands have 16 atoms in their base chains and are located between two identical ones at a distance of  $r = 5$ . The displacements are given in units of the lattice parameter  $a$  of the composite wetting layer, which consists of 10 layers allowed to relax. (b): vertical displacements of the atoms of the central island and of the first layer of the wetting layer for the case of 1 ML-high islands.

clusters instead of a planar film.

We conclude that in the coherent SK growth the incomplete wetting is due to the reduced adhesion of the edge atoms as a result of the lattice misfit. This effect is the TDF for the coherent 3D islanding. The interfacial energy of the boundary between the wetting layer and the 3D crystallites is not zero and cannot be neglected. This is confirmed by the effect of the anharmonicity of the atomic interactions. The stronger repulsive forces between the atoms in the compressed overlayers lead to larger lateral and vertical displacements, and in turn, to weaker wetting in comparison with films that are under tensile stress. Expanded islands adhere stronger to the wetting layer and the TDF is very small to produce 3D islands. As a result, coherent SK growth in expanded films could be expected at very (unrealistically) large absolute values of the negative misfit. The latter, however, depends on the materials parameters (degree of anharmonicity, strength of the chemical bonds, etc.) of the particular system and cannot be completely ruled out. In agreement with the predictions of our model, Xie *et al.* found that  $\text{Si}_{0.5}\text{Ge}_{0.5}$  3D islands are formed on  $\text{Si}_x\text{Ge}_{1-x}$  relaxed buffer layers only under a compressive misfit larger than 1.4 %. Films under tensile stress were always stable against 3D islanding.[25]

A high TDF for coherent 3D islanding requires a large absolute value of the misfit. The sharp increase of the TDF with the misfit in compressed overlayers (Fig. 8) leads to the appearance of a critical misfit beyond which 3D islanding is possible. The existence of a critical misfit clearly shows that the origin of the 3D islanding in the coherent SK growth is the incomplete wetting, which in turn is due to the atomic displacements near the islands edges. Leonard *et al.*[18] have successfully

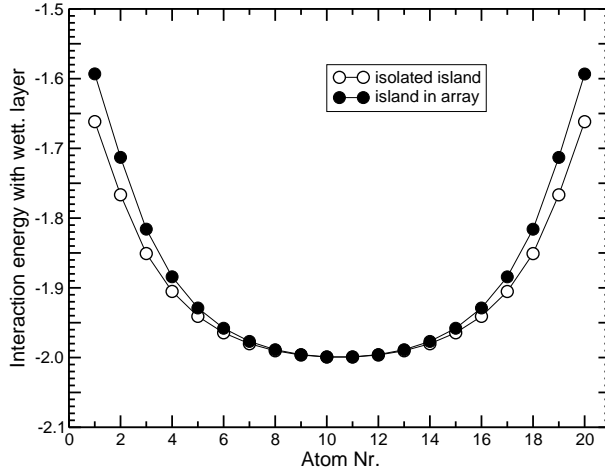


Figure 12: Distribution of the interaction energy (in units of  $V_0$ ) between the atoms of the base chain of a 3 ML-high, coherent island of 20 atoms in the base chain, and the underlying wetting layer, for a positive misfit of 8.0 %. Full circles correspond to an island separated by a distance  $r = 5$  from two identical neighbours, while the empty ones correspond to a reference isolated island.

grown quantum dots of  $\text{In}_x\text{Ga}_{1-x}\text{As}$  on  $\text{GaAs}(001)$  with  $x = 0.5$  ( $\varepsilon_0 \approx 3.6\%$ ) but 60 Å thick 2D quantum wells at  $x = 0.17$  ( $\varepsilon_0 \approx 1.2\%$ ). Walther *et al.*[26] found that the critical In composition is approximately  $x \cong 0.25$ , or  $\varepsilon_0 \cong 1.8\%$ . As mentioned above, a critical misfit of 1.4 % has been found by Xie *et al.* upon deposition of  $\text{Si}_{0.5}\text{Ge}_{0.5}$  films on relaxed buffer layers of  $\text{Si}_x\text{Ge}_{1-x}$  with varying composition.[25]

The increase of  $N_{12}$  with decreasing absolute value of the misfit (Fig. 10) in overlayers under tensile stress is not as sharp as in compressed ones and the critical behaviour is not clearly pronounced in this particular case. Comparing Figs. 8 and 10 clearly shows the reason for this behaviour. Nevertheless, we could expect a critical-like behaviour in experiments. Pinczolits *et al.*[23] have found that deposition of  $\text{PbSe}_{1-x}\text{Te}_x$  on  $\text{PbTe}(111)$  remains purely two dimensional when the misfit is less than 1.6 % in absolute value (Se content < 30%).

In addition to the need of a sufficiently weak adhesion, the existence of a critical misfit appears as a result of the consideration of the island height as a discrete rather than a continuous variable. The latter is also the reason for the complete 2D-3D transformation to pass through a series of intermediate states with discretely increasing thickness. These states are thermodynamically stable in consecutive intervals of the volume. The first step of these transformations is the rearrangement of monolayer-high islands into bilayer islands. Thus the 2D islands appear as natural precursors for the formation of 3D islands beyond some critical size. Moison *et al.* reported a sudden decrease of the surface coverage from 1.75 to 1.2 ML at the moment of formation of InAs 3D islands on GaAs.[12] The same phenomenon has been noticed by Shklyaev *et al.* in the case of Ge/Si(111).[50] Voigtländer and

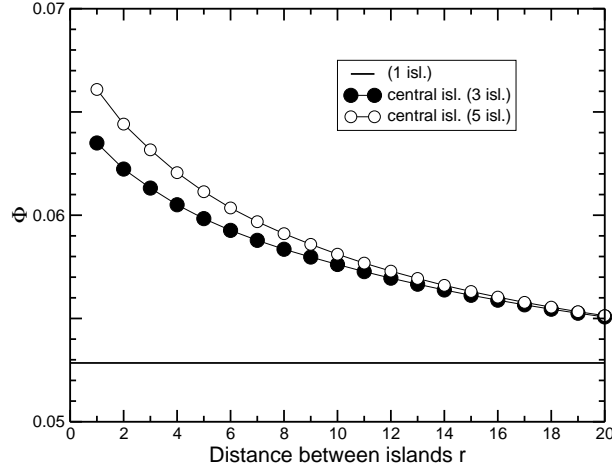


Figure 13: Dependence of the wetting parameter of the central island on the distance  $r$  between the islands. All islands are 3 ML high and have 20 atoms in the base chain. The lattice misfit amounts to 7.0 %. Results for arrays of 3 and 5 islands are given, as well as for a reference isolated island.

Zinner noted that Ge 3D islands in Ge/Si(111) epitaxy have been observed at the same locations where 2D islands locally exceeded the critical wetting layer thickness of 2 bilayers[8]. Ebiko *et al.* found that the volume distribution of InAs/GaAs self-assembled quantum dots agrees well with the scaling function characteristic of monolayer-high islands in submonolayer epitaxy.[51]

The question of the existence and particularly the stability of the intermediate states is more difficult to answer. Rudra *et al.* measured photoluminescence (PL) spectra of InAs layers deposited on InP(001) at two different temperatures (490 and 525°C) and buried in the same material.[27] When the layers were grown at 490°C and the capping layer was deposited immediately after the deposition of the InAs, the spectrum consisted of a single line. If the InAs layer was annealed for 10 s before capping with InP, the spectrum consisted of 8 lines. At 525°C, 3 lines were observed already in absence of annealing. The above observations could be explained by the formation and coexistence of islands with different thickness varying by one monolayer. Colocci *et al.*[28] performed PL studies of InAs deposits on GaAs(001) with thicknesses slightly varying around the critical thickness of 1.6 ML for the onset of the 3D islanding. They observed an increasing number of luminescence lines with increasing film thickness. These lines were attributed to families of 3D islands with similar shape but with heights differing by one monolayer.

Although the above results seem to be in an excellent qualitative agreement with the theoretical predictions of the model, the thermodynamic stability of islands with quantized height of one monolayer, and the existence of a critical misfit is still debated.[1, 52] The reason of the discrepancy of our results with those of Dupont *et al.*[52] most probably stems from the implicit assumption, made by the above

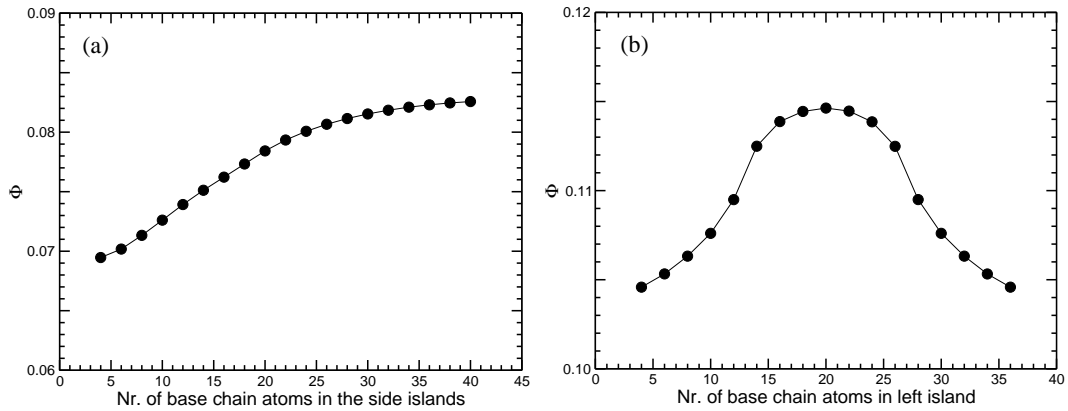


Figure 14: Dependence of the wetting parameter of the central island on the size of the two side islands for two different configurations. In both cases all the islands are 3 ML high, are separated by a distance  $r = 5$  and the central one has 20 atoms in the base chain. In (a) both side islands have equal volumes and the misfit amounts to 7.0 %. In (b), the sum of the volumes of left and right islands is kept constant and equal to the doubled volume of the central island; the misfit is 8.0 %.

authors, that the lengths of the lower ( $R$ ) and the upper ( $R'$ ) bases, and particularly the height ( $h$ ) of the crystal they consider, which has the shape of a frustum of a pyramid, are continuous variables. This is correct if the crystals are sufficiently large. However, the continuum approximation is not acceptable in the beginning of the 2D-3D transformation when the islands are still very small (and thin). It is also not applicable in the limit  $h \ll R$  for the same reason. The problem is in fact analogous to the applicability of the classical nucleation theory to small clusters. A cluster of a given finite size is stable in a finite interval rather than for a fixed value of the supersaturation. These intervals decrease with increasing cluster size and become negligibly small when the clusters are so large that the classical theory of nucleation becomes valid.[36, 53] In the same way the continuum approximation with  $h \ll R$  should be applicable to much larger islands consisting of several million of atoms.

Considering the self-assembly, the presence of neighbouring islands, particularly of those highly compact (with largest angle facets), in the near vicinity of a certain island decreases the adhesion of the latter. The transformation of 2D, monolayer-high islands into bilayer islands takes place by detachment of atoms from the edges and their subsequent jumping and nucleating on the top island's surface.[47] This edge effect shows the influence of the lattice misfit on the rate of second layer nucleation and in turn on the kinetics of the 2D-3D transformation.[54, 55] The presence of neighbouring islands favours the formation of 3D clusters and their further growth. For the self-assembled monodisperse population, the highest tendency to clustering is found.

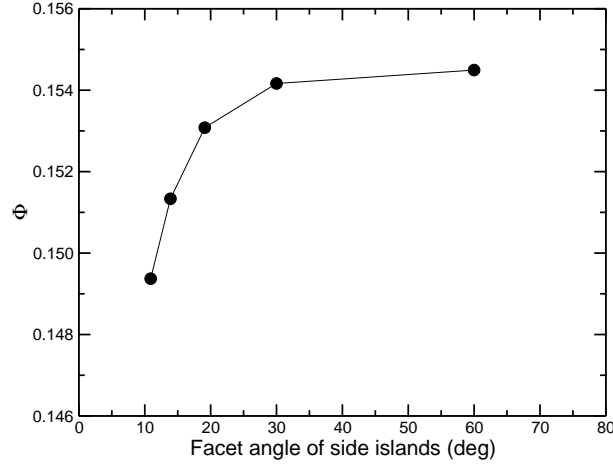


Figure 15: Dependence of the wetting parameter of the central island on the shape of the neighbouring islands, as given by the facet angle of their side walls. The central island has side walls of  $60^\circ$ . All islands are 3 ML high, have 20 atoms in their base chains and are separated by a distance  $r = 5$ . The misfit amounts to 8.0 %.

We can regard the flatter islands in our model ( $11^\circ$  facet angle) as the “hut” clusters discovered by Mo *et al.*, [6] and the clusters with  $60^\circ$  facet angle as the “dome” clusters. It is well known that clusters with steeper side walls relieve the strain more efficiently than flatter clusters [56] (a planar film, the limiting case of the flat islands, does not relieve strain at all). We see that large-angle facet islands affect more strongly the growth of the neighbouring islands, leading to a more narrow size distribution.

Our results lead us to expect a self-assembled population of quantum dots with highest density at low temperatures such that the critical wetting layer thickness for 3D islanding approaches an integer number of MLs. In InAs/GaAs quantum dots the reported values of the critical thickness vary from 1.2 to 2 ML. [17] The critical wetting layer thickness is given by an integer number  $n$  of MLs plus the product of the 2D island density and the critical volume  $N_{12}$  in the  $(n+1)$ -th ML. The 2D island density increases steeply with decreasing temperature. [16] In such a case a dense population of 2D islands will overcome simultaneously the critical size  $N_{12}$  to produce bilayer islands. The value of  $N_{12}$  will be slightly reduced when neighbouring islands are present due to the increase of  $\Phi$ . Regions of high adatom concentrations will favour the highest degree of self-assembly and, due to the larger elastic forces present, are also likely to promote the spatial ordering of the islands, possibly extending to less dense regions and leading to self-organized arrays. Islands will thus interact with each other from the very beginning of the 2D-3D transformation and will give rise to the maximum possible wetting parameter and, in turn, to islands with large-angle facets and a narrow size distribution. This is in agreement with the observations of self-assembled Ge quantum dots on Si(001). [5] At  $700^\circ\text{C}$  a

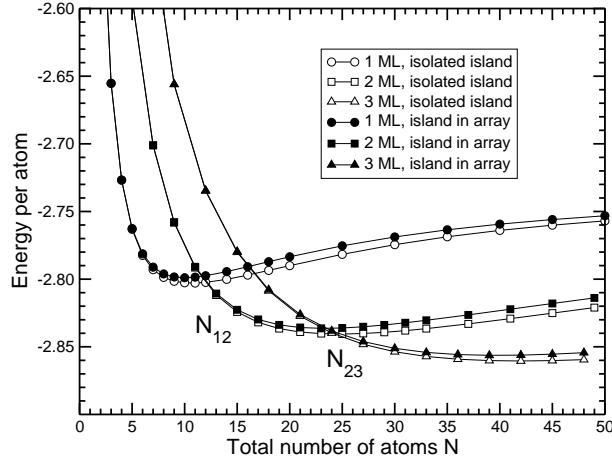


Figure 16: Dependence of the energy per atom, in units of  $V_0$ , on the total number of atoms in compressed coherently strained islands with different thicknesses for a misfit of 7.0 %. The considered island has two identical neighbours at a distance  $n = 5$ . The analogous curves for single isolated islands (empty symbols) are also given for comparison. The wetting layer consists in all cases of 3 ML which are allowed to relax.

population of islands with a concentration ranging from  $10^7$  to  $10^8$   $\text{cm}^{-2}$  is obtained. The islands have the shape of truncated square pyramids with their side wall facets formed by (105) planes (inclination angle of about  $11^\circ$ ). The size distribution of the islands is quite broad. At  $550^\circ\text{C}$  a population of islands with an areal density of the order of  $10^9$  to  $10^{10}$   $\text{cm}^{-2}$  is observed. The islands have larger-angle (113) facets and their size distribution is much more narrow.

Summarizing, the wetting layer and the 3D islands represent different phases which cannot be in equilibrium with each other and the SK morphology is a result of the replacement of one first order phase transition (vapour – wetting layer) by another first order transition (vapour – 3D islands). The transfer of matter from the stable wetting layer to the 3D islands is thermodynamically unfavoured. The experimental observations can be explained on the base of two assumptions: the thermodynamic driving force for the coherent 3D islanding is the incomplete wetting and the height of the 3D islands is a discrete variable varying by one monolayer. This leads to the results that (i) monolayer-high islands with a critical size appear as necessary precursors for 3D islands, (ii) the 2D-3D transition takes place through a series of intermediate states with discretely increasing thickness that are stable in separate intervals of volume (iii) there exists a critical misfit below which coherent 3D islands are thermodynamically unfavoured and the misfit is accommodated by misfit dislocations at a later stage of the growth. Compressed overlayers show a greater tendency to 3D clustering than expanded ones, in agreement with experimental results.

An open question is the mechanism by which the 3D nucleation takes place on top

of the wetting layer. It is well known that a one-dimensional model is inadequate for the treatment of this case, since it will always give a critical nucleus size of one atom.[36] We are confident that in the future, a generalization of our energy minimization model to 2+1 dimensions will allow us to study the 3D nucleation problem in the coherent SK growth.

Finally, the presence of neighbouring islands decreases the wetting of the substrate (in this case the wetting layer) by the 3D islands. The wetting decreases with increasing array density and facet angle of the neighbouring islands. The wetting parameter displays a maximum (implying a minimal wetting) when the array shows a monodisperse size distribution. We expect an optimum self-assembled islanding at low temperatures such that the 2D-3D transformation takes place at the highest possible island density.

#### Acknowledgments

J. E. P. gratefully acknowledges financial support from a “Ramón y Cajal” contract of the Spanish MCyT. E. K. is financially supported by the Spanish MCyT Grant BFM 2001-291-C02-01 and Plan de Promoción de la Investigación UNED’02.

## References

- [1] P. Politi, G. Grenet, A. Marty, A. Ponchet, and J. Villain, *Phys. Rep.* **324**, 271 (2000).
- [2] J. W. Matthews, D. C. Jackson and A. Chambers, *Thin Solid Films* **29**, 129 (1975).
- [3] D. J. Eaglesham and M. Cerullo, *Phys. Rev. Lett.* **64**, 1943 (1990).
- [4] V. A. Shchukin and D. Bimberg, *Rev. Mod. Phys.* **71**, 1125 (1999).
- [5] V. Le Tanh, P. Boucaud, D. Débarre, Y. Zheng, D. Bouchier, and J.-M. Lourtioz, *Phys. Rev. B* **58**, 13115 (1998).
- [6] Y.-W. Mo, D. E. Savage, B. S. Swartzentruber, and M. Lagally, *Phys. Rev. Lett.* **65**, 1020 (1990).
- [7] C. E. Aumann, Y.-W. Mo, and M. Lagally, *Appl. Phys. Lett.* **59**, 1061 (1991).
- [8] B. Voigtländer and A. Zinner, *Appl. Phys. Lett.* **63**, 3055 (1993).
- [9] F. K. LeGoues, M. C. Reuter, J. Tersoff, M. Hammar, and R. M. Tromp, *Phys. Rev. Lett.* **73**, 300 (1994).
- [10] F. M. Ross, J. Tersoff, and R. M. Tromp, *Phys. Rev. Lett.* **80**, 984 (1998).
- [11] M. Kästner and B. Voigtländer, *Phys. Rev. Lett.* **82**, 2745 (1999).

- [12] J. M. Moison, F. Houzay, F. Barthe, L. Leprince, E. André, and O. Vatel, *Appl. Phys. Lett.* **64**, 196 (1994).
- [13] R. Heitz, T. R. Ramachandran, A. Kalburge, Q. Xie, I. Mukhametzhanov, P. Chen, and A. Madhukar, *Phys. Rev. Lett.* **78**, 4071 (1999).
- [14] N. P. Kobayashi, T. R. Ramachandran, P. Chen, and A. Madhukar, *Appl. Phys. Lett.* **68**, 3299 (1996).
- [15] H. Yamaguchi, J. G. Belk, X. M. Zhang, J. L. Sudijono, M. R. Fahy, T. S. Jones, D. W. Pashley, and B. A. Joyce, *Phys. Rev. B* **55**, 1337 (1977).
- [16] B. A. Joyce, J. L. Sudijono, J. G. Belk, H. Yamaguchi, X. M. Zhang, H. T. Dobbs, A. Zangwill, D. D. Vvedensky, and T. S. Jones, *Jpn. J. Appl. Phys.* **36**, 4111 (1997).
- [17] A. Polimeni, A. Patanè, M. Capizzi, F. Martelli, L. Nasi, and G. Salviati, *Phys. Rev. B* **53**, R4213 (1996).
- [18] D. Leonard, M. Krishnamurthy, C. M. Reaves, S. P. Denbaars, and P. M. Petroff, *Appl. Phys. Lett.* **63**, 3203 (1993).
- [19] S. Guha, A. Madhukar, and K. C. Rajkumar, *Appl. Phys. Lett.* **57**, 2110 (1990).
- [20] C. W. Sneider, B. G. Orr, D. Kessler, and L. M. Sander, *Phys. Rev. Lett.* **66**, 3032 (1991).
- [21] J. Temmyo, R. Nötzel, and T. Tamamura, *Appl. Surf. Sci.* **121/122**, 63 (1997).
- [22] N. Carlsson, W. Seifert, A. Peterson, P. Castrillo, M. E. Pistol, and L. Samuelson, *Appl. Phys. Lett.* **65**, 3093 (1994).
- [23] M. Pinczolits, G. Springholz, and G. Bauer, *Appl. Phys. Lett.* **73**, 250 (1998).
- [24] R. Peierls, *Phys. Rev. B* **18**, 2013 (1978).
- [25] Y. H. Xie, G. H. Gilmer, C. Roland, P. J. Silverman, S. K. Buratto, J. Y. Cheng, E. A. Fitzgerald, A. R. Kortan, S. Schuppler, M. A. Marcus, and P. H. Citrin, *Phys. Rev. Lett.* **73**, 3006, (1994).
- [26] T. Walther, A. G. Cullis, D. J. Norris, and M. Hopkinson, *Phys. Rev. Lett.* **86**, 2381 (2001).
- [27] A. Rudra, R. Houdré, J. F. Carlin, and M. Ilegems, *J. Cryst. Growth* **136**, 278 (1994); R. Houdré, J. F. Carlin, A. Rudra, J. Ling, and M. Ilegems, *Superlattices and Microstructures* **13**, 67 (1993).
- [28] M. Colocci, F. Bogani, L. Carraresi, R. Mattolini, A. Bosacchi, S. Franchi, P. Frigeri, M. Rosa-Clot, and S. Taddei, *Appl. Phys. Lett.* **70**, 3140 (1997).

- [29] J. Tersoff and R. M. Tromp, *Phys. Rev. Lett.* **70**, 2782 (1993); J. Tersoff and F. K. LeGoues, *Phys. Rev. Lett.* **72**, 3570 (1994).
- [30] M. Grundmann, J. Christen, N. N. Ledentsov, J. Böhrer, D. Bimberg, S. S. Ruvimov, P. Werner, U. Richter, U. Gösele, J. Heydenreich, V. M. Ustinov, A. Yu. Egorov, A. E. Zhukov, P. S. Kop'ev, and Zh. I. Alferov *Phys. Rev. Lett.* **74**, 4043 (1995).
- [31] Z. Jiang, H. Zhu, F. Lu, J. Qin, D. Huang, X. Wang, C. Hu, Y. Chen, Z. Zhu, and T. Yao, *Thin Solid Films* **321**, 60 (1998).
- [32] C. Teichert, *Phys. Rep.* **365**, 335 (2002).
- [33] R. Kern, G. LeLay, and J. J. Metois, in *Current Topics in Mater. Sci.*, Vol. 3, ed. by E. Kaldis, (North-Holland, 1979).
- [34] S. Stoyanov, *Surf. Sci.* **172**, 198 (1986).
- [35] I. Markov and S. Stoyanov, *Contemp. Phys.* **28**, 267 (1987).
- [36] I. Markov, *Crystal Growth for Beginners*, 2nd edition, (World Scientific, 2003).
- [37] W. Kossel, *Nachrichten der Gesellschaft der Wissenschaften Göttingen, Mathematisch-Physikalische Klasse*, Band 135 (1927).
- [38] I. N. Stranski, *Z. Phys. Chem.* **136**, 259 (1928).
- [39] E. Bauer, *Z. Kristallographie* **110**, 372 (1958).
- [40] J. E. Prieto and I. Markov, *Phys. Rev. B* **66**, 073408 (2002).
- [41] E. Korutcheva, A. M. Turiel, and I. Markov, *Phys. Rev. B* **61**, 16890 (2000).
- [42] C. Ratsch and A. Zangwill, *Surf. Sci.* **293**, 123 (1993).
- [43] Ya. I. Frenkel and T. Kontorova, *J. Phys. Acad. Sci. USSR* **1**, 137 (1939).
- [44] I. Markov, *Phys. Rev. B* **48**, 14016 (1993).
- [45] F. C. Frank and J. H. van der Merwe, *Proc. Roy. Soc. London, Ser. A* **198**, 205 (1949); **198**, 216 (1949).
- [46] J. H. van der Merwe, J. Woltersdorf, and W. A. Jesser, *Mater. Sci. Eng.* **81**, 1 (1986).
- [47] S. Stoyanov and I. Markov, *Surf. Sci.* **116**, 313 (1982).
- [48] I. Markov and J. E. Prieto, in *Atomistic Aspects of Epitaxial Growth*, Vol. 65 of *NATO Science Series, II*, eds. M. Kotrla, N.I. Papanicolaou, D.D. Vvedensky and L.T. Wille, 441 (Kluwer, 2002).

- [49] O. V. Lysenko, V. S. Stepanyuk, W. Hergert, and J. Kirschner, *Phys. Rev. Lett.* **89**, 126102 (2002).
- [50] A. Shklyaev, M. Shibata, and M. Ichikawa, *Surf. Sci.* **416**, 192 (1998).
- [51] Y. Ebiko, S. Muto, D. Suzuki, S. Itoh, H. Yamakoshi, K. Shiramine, T. Haga, K. Unno and M. Ikeda, *Phys. Rev. B* **60**, 8234 (1999).
- [52] C. Duport, C. Priester, and J. Villain, in *Morphological Organization in Epitaxial Growth and Removal*, Vol. 14 of *Directions in Condensed Matter Physics*, edited by Z. Zhang and M. Lagally (World Scientific, Singapore, 1998).
- [53] A. Milchev and J. Malinowski, *Surf. Sci.* **156**, 36 (1985).
- [54] S. N. Filimonov and Yu. Yu. Hervieu, *Surf. Sci.* **507-510**, 270 (2002).
- [55] C. H. Lin and Y.-C. Tsai, *Surf. Sci.* **512**, 287 (2002).
- [56] M. Horn-von Hoegen, *Surf. Sci.* **537**, 1 (2003).